

# Electrical characterization of organic resistive memory with interfacial oxide layers formed by O<sub>2</sub> plasma treatment

Byungjin Cho, Sunghoon Song, Yongsung Ji, and Takhee Lee<sup>a)</sup>

*Department of Materials Science and Engineering, Department of Nanobio Materials and Electronics, Gwangju Institute of Science and Technology, Gwangju 500-712, Republic of Korea*

(Received 6 June 2010; accepted 23 July 2010; published online 13 August 2010)

We studied organic resistive memory devices with interfacial oxide layers, the thickness of which depended on O<sub>2</sub> plasma treatment time. The different interfacial oxide thicknesses sequentially changed the ON and OFF states of the final memory devices. We found that the memory devices that had undergone additional plasma treatment showed higher ON/OFF ratios than devices without the treatment, which was due to the relatively large OFF resistance values. However, a long oxidation process widened the threshold voltage distribution and degraded the switching reproducibility. This indicates that the oxidation process should be carefully optimized to provide practical high-performance organic memory. © 2010 American Institute of Physics. [doi:10.1063/1.3478840]

Organic resistive memory has attracted a significant amount of attention because of its attractive features which include low-cost processing, printability, and flexibility.<sup>1-6</sup> Because of these merits, various organic materials such as molecules, polymers, and composites have been extensively employed as the active layers in organic memory devices.<sup>1,4,7</sup> The research interest has mainly been focused on the development of new organic memory materials. However, the interface states between the electrode and the organic film have been considered an important factor in terms of the performance of organic electronics such as organic photovoltaic cells, organic light-emitting diodes, and organic thin-film transistors.<sup>8</sup> There are a few reports about organic memory that address interface engineering.<sup>9,10</sup> For instance, the ON/OFF ratio is significantly enhanced by introducing Ag nanodots between the organic layer and an indium tin oxide surface; the nanodots act as charge-trapping sites.<sup>9</sup> Also, self-assembled monolayer treatment on the electrode enhances the switching reproducibility by improving the current level distribution.<sup>10</sup> In particular, we note that naturally formed native oxides on an Al surface strongly influence the switching characteristics,<sup>11,12</sup> and reproducible switching in organic memory can be realized through the intentional introduction of an additional oxide film.<sup>13</sup> Nevertheless, there have been few detailed studies on the effects of an interfacial oxide on the various switching parameters and performance (ON/OFF ratio, threshold voltage, endurance, and retention). Furthermore, O<sub>2</sub> plasma treatment would be highly preferable because of a cost-effective method to form the interfacial oxide.

In this paper, we investigated the resistive switching characteristics of organic memory devices with interfacial oxides formed using an O<sub>2</sub> plasma treatment method. The devices treated with plasma generally showed higher ON/OFF ratios than devices without the O<sub>2</sub> plasma treatment. However, the threshold voltage distribution and switching reproducibility were degraded in devices with longer treatment times. Considering these various memory parameters, the oxidation process should be carefully performed and optimized.

The organic resistive memory consisted of a composite material of polyimide (PI) and [6,6]-phenyl-C61 butyric acid methyl ester (PCBM) (denoted as PI:PCBM) sandwiched between Al electrodes. To make an active layer of organic resistive memory, biphenyltetracarboxylic acid dianhydride p-phenylene diamine (BPDA-PPD), used as a PI precursor, was dissolved in N-methyl-2-pyrrolidone (NMP) (BPDA-PPD:NMP solvent=1:4 weight ratio). PCBM was also dissolved in NMP at a concentration of 0.5 wt %. A PI:PCBM blending solution was then prepared by mixing the PI solution (2 ml) with the PCBM solution (0.5 ml). Bottom Al electrodes (50 nm thick) with eight line patterns were deposited using a shadow mask. To create an additional Al oxide layer, the bottom electrodes were treated with O<sub>2</sub> plasma [rf power: 100 W; O<sub>2</sub>: 30 SCCM (SCCM denotes cubic centimeter per minute at STP); and treatment time: 0, 5, 10, and 20 min]. The Al oxide surface was also exposed to UV-ozone for 10 min to improve the reliability of the organic resistive memory.<sup>13</sup> The PI:PCBM composite solution was then spin coated over the bottom electrodes at 2000 rpm for 40 s. The coated film was soft baked at 120 °C on a hotplate for 10 min to evaporate the solvent and then thermally cured at 300 °C under a nitrogen atmosphere for 30 min. The thickness of the PI:PCBM composite layer was measured to be ~20 nm by transmission electron microscopy (TEM). To form the top electrodes, a shadow mask with eight line patterns was vertically aligned on the bottom Al lines and a 50-nm-thick Al layer was deposited using an e-beam evaporator. A completed organic memory device had an 8×8 crossbar array structure with a junction area of 100 × 100 μm<sup>2</sup>. All electrical measurements were performed using a semiconductor characterization system (Keithley 4200-SCS) at room temperature in a N<sub>2</sub>-filled glove box.

Figure 1(a) illustrates a schematic of the organic memory devices with 8×8 cells that consist of Al/PI:PCBM/Al layers. As shown in Fig. 1(b), the oxide thickness on the bottom Al electrodes varied as a function of the O<sub>2</sub> plasma treatment time (0, 5, 10, and 20 min). The dispersion of the oxide thickness values was plotted by taking the statistical average and the standard error (SE=s/√n where s and n denote the standard deviation and the number of data points, respectively) of data sets measured from the TEM images of individual devices. Even the device with no treat-

<sup>a)</sup>Electronic mail: tlee@gist.ac.kr.

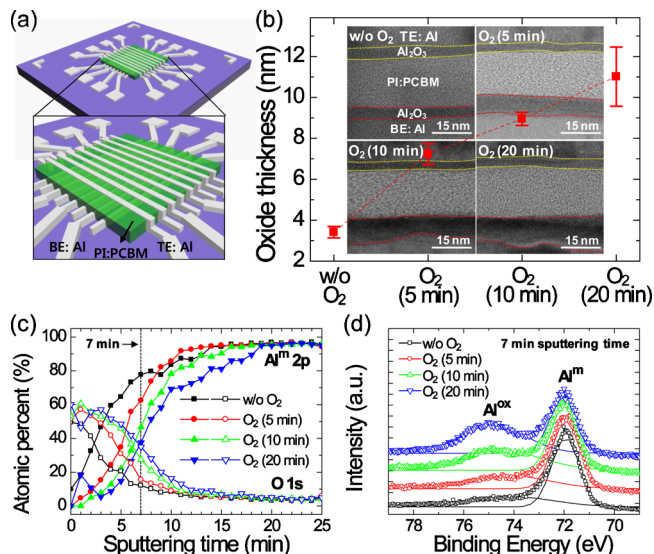


FIG. 1. (Color online) (a) A schematic of the Al/PI:PCBM/Al organic resistive memory with an  $8 \times 8$  array of cells. (b) The thickness of Al oxide as a function of the  $O_2$  plasma treatment time: 0, 5, 10, and 20 min. The insets show TEM images of each memory device. The yellow and red dotted lines indicate the native Al oxide formed during the deposition of the top electrodes and the interfacial Al oxide with varying thicknesses on the bottom electrodes created by the plasma treatment, respectively. (c) The XPS depth profile of  $Al^{m} 2p$  and  $O 1s$  in the Al samples that were treated for varying times with an  $O_2$  plasma. (d) A comparison of the XPS spectra of the  $Al^{ox}$  and  $Al^{m}$  peaks after 7 min of sputtering for the four types of Al samples.

ment had a thin native oxide film ( $\sim 3.5$  nm thick) naturally formed by residual oxygen gas inside the deposition chamber. The oxide thickness gradually increased with the treatment time. The increasing amounts of oxide resulted from the time-induced enhancement of chemical reactions between Al atoms and oxygen molecules. As the treatment time increased, the interface quality between the Al and the oxide seemed to become worse.

To quantitatively compare the elements of the samples based on plasma exposure time, we analyzed the x-ray photoelectron spectroscopy (XPS) depth profiles of the Al samples treated with  $O_2$  plasma for different lengths of time (0, 5, 10, and 20 min). Figure 1(c) shows the XPS depth profiles of the samples where  $Al^{m} 2p$  and  $O 1s$  correspond to the metallic Al peak (Al–Al bonds) and the oxygen peak (Al–O bonds), respectively. With plasma treatment time increased, the amount of the oxygen atoms gradually increased throughout the total depth and the amount of the Al atoms decreased. Naturally, 20 min of plasma treatment led to the highest oxygen and lowest Al atomic percent values, indicating considerable diffusion of oxygen gas into the Al layer. The diffused oxygen gas contributed to the formation of Al oxide.

We analyzed the Al  $2p$  peak of the XPS spectra of all of the samples after 7 min of sputtering (near a depth of  $\sim 13$  nm), as shown in Fig. 1(d). Each spectrum was offset vertically for better distinction. The spectra of the Al  $2p$  region clearly showed both the  $Al^{m}$  (binding energy of 72.0 eV) and  $Al^{ox}$  (binding energy of 74.5 eV) peaks; the two markers correspond to metallic Al and oxygen-bonded Al, respectively.<sup>14,15</sup> The relative intensity of the  $Al^{ox}$  peak to the  $Al^{m}$  peak gradually increased with an increase in the plasma treatment time. A longer  $O_2$  plasma treatment time resulted in more chemical bonding between Al atoms and oxygen

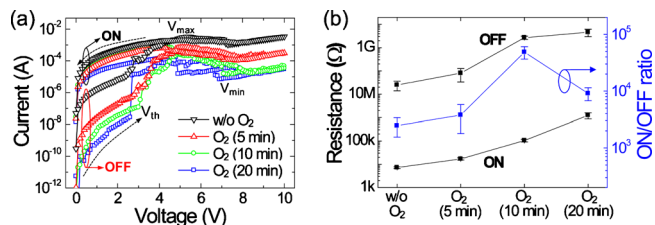


FIG. 2. (Color online) (a) I-V characteristics of organic memory devices treated with an  $O_2$  plasma for different lengths of time. (b) The ON and OFF resistances (left y-axis) and the ON/OFF ratios (right y-axis) as a function of the  $O_2$  plasma treatment time.

molecules, thereby generating a thicker Al oxide layer. This result was consistent with the TEM data in Fig. 1(b).

Figure 2(a) shows the current-voltage (I-V) characteristics of four types of organic memory devices measured on the bottom electrodes that were treated for different times with  $O_2$  plasma (0, 5, 10, or 20 min). After forming process, the devices were switched reversibly between a high and low resistance state. All of the devices showed typical unipolar switching behavior, which is achieved through the successive application of voltage with the same polarity.<sup>16</sup> However, the electrical current levels were different, depending on the plasma treatment time. In particular, the OFF states of the organic memory devices changed more than the ON states. The devices were programmed from an initial high resistance state (OFF state) to a low resistance state (ON state) at the threshold voltages ( $V_{th}$ ). When the voltage was increased further, the device current gradually decreased to a minimum value at  $V_{min}$ , indicating a negative differential resistance. However, the devices could be erased with an applied voltage above the  $V_{min}$ . During sweeping back to 0 V, the current followed the upper curve and the device remained in the ON state. From these results, the operating voltages for writing, erasing, and reading were determined to be  $\sim 5$  V, 10 V, and 0.5 V, respectively. Especially, positive voltages were applied to the top electrode for the resistive switching of our memory devices while the bottom electrode was grounded. These resistive switching phenomena may be associated with the charge-trapping/detrapping mechanism described by Simmons and Verderber<sup>17</sup> and Bozano *et al.*<sup>7,18</sup>

The ON and OFF resistances of each device as a function of the plasma treatment time were compared and are shown on the left y-axis of Fig. 2(b). The dispersion of the resistance values was obtained by taking the statistical average and standard error of sets of individual memory cells (more than 30 cells at each data point). Both the ON and OFF resistance values gradually increased with the plasma treatment time. Compared with the ON resistances, a relatively large increase in OFF resistances contributed to a higher ON/OFF ratio compared with the devices without  $O_2$  plasma treatment. This indicated that the additional oxide served as a series resistor and greatly affected the initial OFF resistance. In particular, the highest ON/OFF ratio of over  $10^4$  was obtained in the devices treated for 10 min with  $O_2$  plasma, as shown on the right y-axis of Fig. 2(b). The OFF resistances did not seem to increase further in the devices with 20 min of plasma treatment, which eventually exhibited a decrease in the ON/OFF ratio.

The statistical data of the threshold voltages were extracted from 33 randomly selected cells in each organic memory device. Figure 3(a) shows the threshold voltage his-

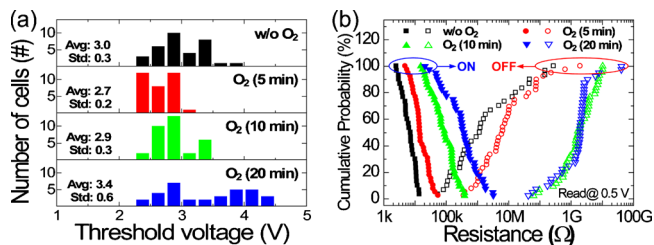


FIG. 3. (Color online) (a) The threshold voltage distributions of organic memory devices treated with an  $O_2$  plasma for different lengths of time. (b) The cumulative probability data of each ON and OFF resistance for the organic memory devices treated with an  $O_2$  plasma for different lengths of time.

tograms for sets of each device. Almost the same voltage distribution was observed in the three types of devices (0, 5, and 10 min) treated with plasma for 10 min or less. On the other hand, the devices treated with plasma for 20 min showed a relatively wide voltage distribution, as confirmed by the large value of the standard deviation. The forming voltages or switching voltages of the organic memory devices are critically dependent on the properties of both the active materials and their interfaces.<sup>10,13,19</sup> This difference may be associated with the relatively thick and rough interfacial oxide of the device with longer plasma treatment, as observed in the TEM image in Fig. 1(b). Unfortunately, the wide threshold voltage distribution often leads to failure in programming the cell. Thus, the plasma treatment time and conditions should be carefully executed to prevent switching failure.

It is important to investigate cell-to-cell uniformity for practical memory applications. Figure 3(b) shows the cumulative probability data for the ON and OFF resistance values obtained from more than 30 cells in each device. All memory devices showed reasonably good separation between the ON and OFF states without any overlap. The device treated with  $O_2$  plasma for 10 min was the best candidate for practical organic memory applications because it had the largest gap between the ON and OFF distribution.

The performance of each memory device was evaluated and compared in terms of endurance cycles and retention time. The endurance cycling test was carried out by repetitive sweeping operations of a single cell [Fig. 4(a)]. During 150 sweep cycles, the two current states of each device remained stable without any serious electrical degradation. However, the device treated with plasma for 20 min showed large fluctuations in the ON resistance values, which may have been caused by the poor quality of the oxide interface, as documented in the TEM image. A large number of defect states at the interface give rise to unintentional charge trap-

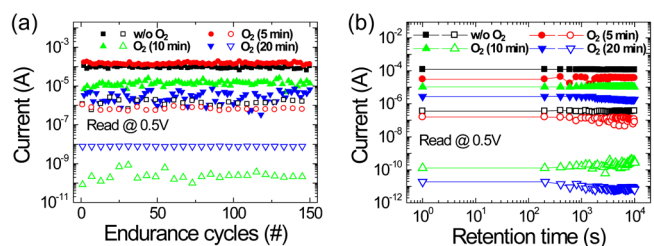


FIG. 4. (Color online) (a) The endurance cycles of the four types of organic memory devices. (b) The retention times of the four types of organic memory devices.

ping, which results in unstable charge transport through the interface.

To evaluate the ability to retain information, we also tested the retention times of the ON and OFF states of each device shown in Fig. 4(b). Each device presented long retention characteristics of up to  $10^4$  sec, indicating a stable information storage capability. Even though we did observe a small amount of degradation in the ON state in the device treated with plasma for 20 min, it was negligible because the ON/OFF ratio was large enough to cover the retention degradation.

In conclusion, we investigated organic resistive memory devices with interfacial oxide layers created using a simple  $O_2$  plasma treatment method. The interfacial oxide thickness increased with the plasma treatment time, which in turn changed the bistable resistance values. The devices subjected to additional plasma treatment exhibited higher ON/OFF ratios than devices with only native oxide, however, the threshold voltage distribution and switching reproducibility degraded in devices subjected to long plasma treatment times. Thus, the  $O_2$  plasma treatment conditions for the oxide formation should be carefully optimized by considering the essential memory parameters such as ON/OFF ratio, threshold voltage, and switching reproducibility.

This work was supported by the National Research Laboratory program, National Core Research Center grant, World Class University program of the Korean Ministry of Education, Science and Technology, the Program for Integrated Molecular Systems/GIST, and the IT R&D program of MKE/KEIT.

<sup>1</sup>C. P. Collier, G. Mattersteig, E. W. Wong, Y. Luo, K. Beverly, J. Sampaio, F. M. Raymo, J. F. Stoddart, and J. R. Heath, *Science* **289**, 1172 (2000).

<sup>2</sup>S. Möller, C. Perlov, W. Jackson, C. Taussig, and S. R. Forrest, *Nature (London)* **426**, 166 (2003).

<sup>3</sup>J. C. Scott and L. D. Bozano, *Adv. Mater.* **19**, 1452 (2007).

<sup>4</sup>Q.-D. Ling, D.-J. Liaw, C. Zhu, D. S.-H. Chan, E.-T. Kang, and K.-G. Neoh, *Prog. Polym. Sci.* **33**, 917 (2008).

<sup>5</sup>T.-W. Kim, H. Choi, S.-H. Oh, G. Wang, D.-Y. Kim, H. Hwang, and T. Lee, *Adv. Mater.* **21**, 2497 (2009).

<sup>6</sup>B. Cho, T.-W. Kim, S. Song, Y. Ji, M. Jo, H. Hwang, G.-Y. Jung, and T. Lee, *Adv. Mater.* **22**, 1228 (2010).

<sup>7</sup>L. D. Bozano, B. W. Kean, M. Beinhoff, K. R. Carter, P. M. Rice, and J. C. Scott, *Adv. Funct. Mater.* **15**, 1933 (2005).

<sup>8</sup>H. Ma, H.-L. Yip, F. Huang, and A. K.-Y. Jen, *Adv. Funct. Mater.* **20**, 1371 (2010).

<sup>9</sup>T. Kondo, S. M. Lee, M. Malicki, B. Domercq, S. R. Marder, and B. Kippelen, *Adv. Funct. Mater.* **18**, 1112 (2008).

<sup>10</sup>B.-O. Cho, T. Yasue, H. Yoon, M.-S. Lee, I.-S. Yeo, U. I. Chung, J.-T. Moon, and B.-I. Ryu, *Tech. Dig. - Int. Electron Devices Meet.* **2006**, 781.

<sup>11</sup>M. Cölle, M. Büchel, and D. M. de Leeuw, *Org. Electron.* **7**, 305 (2006).

<sup>12</sup>K. S. Yook, J. Y. Lee, S. H. Kim, and J. Jang, *Appl. Phys. Lett.* **92**, 223305 (2008).

<sup>13</sup>F. Verbakel, S. C. J. Meskers, R. A. J. Janssen, H. L. Gomes, M. Cölle, M. Büchel, and D. M. de Leeuw, *Appl. Phys. Lett.* **91**, 192103 (2007).

<sup>14</sup>M. Chen, X. Wang, Y. H. Yu, Z. L. Pei, X. D. Bai, C. Sun, R. F. Huang, and L. S. Wen, *Appl. Surf. Sci.* **158**, 134 (2000).

<sup>15</sup>S. Gredeļ, A. R. Gerson, S. Kumar, and G. P. Cavallaro, *Appl. Surf. Sci.* **174**, 240 (2001).

<sup>16</sup>B. Cho, T.-W. Kim, M. Choe, G. Wang, S. Song, and T. Lee, *Org. Electron.* **10**, 473 (2009).

<sup>17</sup>J. G. Simmons and R. R. Verderber, *Proc. R. Soc. London, Ser. A* **301**, 77 (1967).

<sup>18</sup>L. D. Bozano, B. W. Kean, V. R. Deline, J. R. Salem, and J. C. Scott, *Appl. Phys. Lett.* **84**, 607 (2004).

<sup>19</sup>W.-J. Joo, T.-L. Choi, K.-H. Lee, and Y. Chung, *J. Phys. Chem. B* **111**, 7756 (2007).